International RILEM Conference on Materials, Systems and Structures in Civil Engineering
Conference segment on Concrete with Supplementary Cementitious Materials
22-24 August 2016, Technical University of Denmark, Lyngby, Denmark

CARBONATION MECHANISM OF DIFFERENT KINDS OF C-S-H: RATE AND PRODUCTS

Bei Wu [(1)], Guang Ye [(1,2)]

(1) Microlab, Delft University of Technology, 2628 CN, Delft, The Netherlands
(2) Magnel Laboratory for Concrete Research, Ghent University, 9052 Ghent, Belgium

Abstract
During the carbonation of cement paste blended with supplementary cementitious materials, the C-S-H with different Ca/Si ratios, formed from the hydration and pozzolanic reactions, are the major calcium-bearing phases which react with CO_2. Therefore, it's important to study the carbonation mechanism of different C-S-H phases. In this paper, the pure C-S-H phases (Ca/Si ratio: 0.66 to 2.0) were synthesized and used for the accelerated carbonation test. Synthesized C-S-H phases with different Ca/Si ratio were identified by X-ray diffraction and ^{29}Si nuclear magnetic resonance. The carbonation rate and products of different C-S-H phases are also determined. The results show that pure C-S-H phases with different Ca/Si ratio (lower than 1.40) can be synthesized in the lab. The structure of synthesized C-S-H is similar to the C-S-H(I) reported by Taylor. The mean chain length of the C-S-H decreases dramatically when the Ca/Si ratio increases from 0.66 to 1.40, then it keeps no change. The portlandite appears in the products when the designed Ca/Si ratio is over 1.40. The C-S-H with lower Ca/Si ratio is decomposed faster than that with a higher Ca/Si ratio. All the C-S-H phases are fully decomposed to $CaCO_3$ and silica gel after 3 days' accelerated carbonation.

1. Introduction

Carbonation of C-S-H has been studied by many authors [1, 2]. It is a complex decalcification-polymerization process of the C-S-H and the formation of amorphous silica gel, see Eq. (1).

$$C_xSH_y + x\overline{C} \rightarrow xC\overline{C} + SH_t + (y-t)H \quad (1)$$

It is reclaimed that, in cement notations, $C = CaO$, $H = H_2O$, $S = SiO_2$, $A = Al_2O_3$, and $\overline{C} = CO_2$. x, y and t are the molecular numbers. According to the Eq. (1), the carbonation mechanism, like reaction rate and products, depends on the properties of C-S-H like Ca/Si

(C/S) and H_2O/Si (H/S). It is better to study the carbonation mechanism of C-S-H on the basis of the C-S-H structure.

The C-S-H phase has a layer structure can be inferred from the refined structure of 11Å tobermorite ($Ca_{4.5}Si_6O_{16}(OH)\cdot 5H_2O$) [3]. The layer structure of 11Å tobermorites consists of three parts: CaO_2 sheet, 'dreierkette' form SiO chain and interlayer, illustrated in Fig. 1a. In the CaO_2 sheet layer, the 7-fold coordinated Ca^{2+} share all the oxygen atoms with Si^{4+} in SiO chains of SiO_4 tetrahedra on both side of the CaO_2 layer. In the SiO chain layer, SiO_4 tetrahedra coordinate themselves to Ca ions by linking in a dreierketten arrangement, to repeat a kinked pattern after three tetrahedra[4]. Two of the tetrahedra are linked to CaO polyhedral by sharing O-O edges with the central Ca-O part of the layer, called paired tetrahedra (PT); the third tetrahedra shares an oxygen atom at the pyramidal apex of a Ca polyhedron, called bridging tetrahedra (BT). There are Ca^{2+} cations and water molecules in the interlayer.

Comparing with the tobermorites, the major difference of the structure of C-S-H in Portland cement concrete, is that the chains of SiO_4 tetrahedra are broken. The C-S-H contains dimeric, pentameric and even higher polymeric species of SiO_4 tertrahedra, resulting in chains of 2, 5, …, (3n-1) SiO_4 tetrahedra. It is proved by experimental studies[5-7] and molecular modeling research[8]. Fig. 1a illustrates the pentameric unit, in which a bridging SiO_4 (Q_B^2) connects two dimers, resulting in two SiO_4 end-groups (Q^1) and two 'paired' SiO_4 sites (Q_P^2). Normally, the Q_3 or Q_4 SiO_4 tetrahedra is absent in the C-S-H produced by the Portland cement hydration.

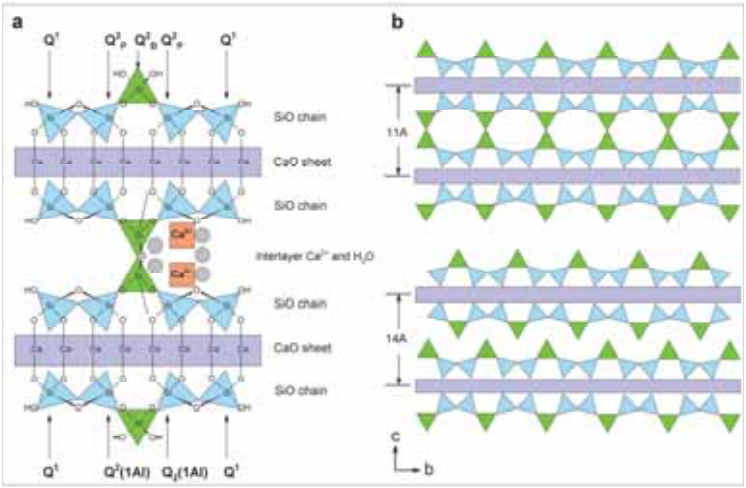

Figure 1 Schematic of the layer crystal structure for the 11 Å tobermorite. The upper part shows different types of SiO4 tetrahedra in a pure pentameric silicate chain, which is a characteristic feature of the 'dreierketten'-based models for the C-S-H phase. The lower part illustrates the possible incorporation of Al in the bridging site and the formation of Q2(1Al) tertrahedra in C-(A-)S-H. b. Comparing between the interlayer structures of 11 Å tobermorite and 14 Å tobermorite.

The C/S of C-S-H in the concrete is normally higher than 0.83. The increase of the C/S in C-S-H based on the tobermorite structure can be caused by: omission of the bridge tetrahedra and incorporation of additional calcium in the interlayer. If all the bridge tetrahedra are removed, the C/S can increase to 1.25[9, 10]. Further incorporation of extra Ca^{2+} in the interlayer can form the C-S-H with a much higher C/S. The theoretical value is 1.50 when all the bridge sites are removed and taken up by extra Ca^{2+}[9]. The extra Ca^{2+} is normally balanced by the omission of H^+ or the incorporation of OH^- or both. If the amount of extra Ca continues increasing and achieves a C/S even higher than 1.5, the structure of C-S-H is more close to the C-S-H/CH 'solid solution' (T/CH model)[9].

From the above discussion, three types of Ca exist in the C-S-H structure (classification by the position of Ca): Ca in the CaO_2 sheet layer, Ca in the interlayer, Ca from the CH in the 'solid solution'. The proportion of them varies from C-S-H to C-S-H. Apparently, to remove the Ca from the above three chemical site needs different energy, which means the decalcification rate are different among C-S-H phases. Moreover, the removal of Ca in the latter two site causes less changes of the structure than that in the CaO_2 sheet layer. This is why the decalcification of C-S-H may cause the shrinkage of cement paste, especially for the C-S-H with Ca/Si lower than 1.2 [11].

The aim of this work is to synthesize the single C-S-H phase with different C/S and study their carbonation rate and products. Base on this, to explain the phase transformation and microstructure development of blended cement paste during the carbonation, discovered in the former research [12].

2. Experiments and test methods

2.1. Raw Materials

The raw materials used in the synthesis are CaO and fumed silica. CaO is freshly prepared by the calcination of $CaCO_3$ under 1000 °C for at least 4 hours before synthesis. Fumed silica is from Sigma-Aldrich, with the surface area of 175-225 m^2/g.

2.2. Synthesis of C-S-H with different C/S

C-S-H gels were prepared by using stoichiometric amounts of CaO and fumed silica, to give approximate C/S ranging between 0.66 and 2.0. The solid phases were mixed together with CO_2-free water. The water/solid ratio was 50:1. The solution was stirred by magnetic stirrer at around 20 °C. The whole synthesis procedure was under N_2 protection in case of carbonation. After 2 or 4 weeks' reaction, samples of solid and liquid were extracted as a slurry. Solids were obtained by filtering the slurries through a Balston No. 45 paper. Then they were quickly moved into the vacuum drying chamber and dried under 35 °C for 24 h. Then the sample was stored in the desiccator with the relative humidity of 30%, controlling by the standard saturated $CaCl_2 \cdot 6H_2O$ solution. The set-up of the synthesis device is illustrated in Fig.2. The mix design of different C-S-H is described in Tab. 1.

2.3. Accelerated carbonation of C-S-H

Well-dried C-S-H samples were grinded into powders and moved into a carbonation chamber. The CO_2 concentration is maintained at 3% ± 0.2 automatically by the solenoid valve

connected with a CO_2 sensor. The temperature is regulated at 20 °C and the relative humidity is controlled at around 75% by using the saturated NaCl solution). The carbonation time varies from 0.5 h to 7 days.

2.4. Test methods

Test methods used for the identification of different types of C-S-H and the carbonation products were X-ray diffraction (XRD), Fourier transform infrared spectroscopy (FTIR) and nuclear magnetic resonance (NMR). Major crystalline phases in the products were tested by XRD. The X-ray source used is Cu K radiation (λ = 0.154056 nm, 60 mA, 40 KV). The scan step size was 0.02°, from 5° to 70° (2θ). The scan time per step is 8 s. The FTIR spectra were collected over the wavelength range of 4000 to 400 cm^{-1} by the TM 100 Optical ATR-FTIR spectrometer. The resolution was 4 cm^{-1}. The samples were grinded into powders with same fineness as that required for the XRD test.

Solid state ^{29}Si single pulse magic angle spinning (MAS) NMR spectra were acquired using a BrukerMSL-400 spectrometer (magnetic field of 9.8 T; operating frequencies of 79.5 MHz). C-S-H powders were packed into the zirconia rotor sealed at either end with Teflon end plugs, and spun at 6 kHz in a Varian 7 mm wide-body probe. The spectra were acquired using a pulse recycle delay of 5 s, a pulse width of 4.97 μs, and an acquisition time of 20 ms; 2002 scans were collected for each sample. ^{29}Si chemical shifts are given relative to tetrakis (trimethylsilyl) silane (TTMS) at -9.8 ppm, with kaolinite as an external standard at - 91.2 ppm.

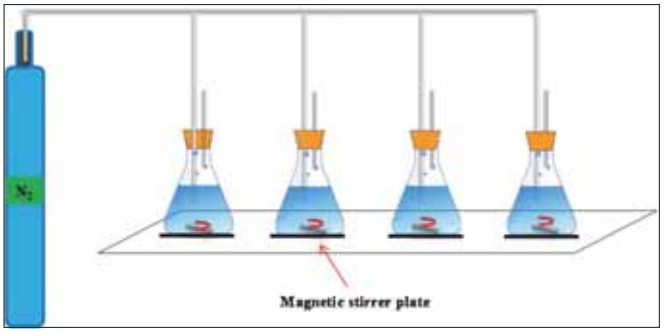

Figure 2 Schematic diagram of the synthesis set-up

Table 1 Mass fraction of raw materials for preparing different C-S-H

Sample NO.	Ca/Si ratio	CaO (g)	SiO_2(g)	H_2O (g)
1	0.66	3.0	4.9	400
2	0.86	3.6	4.4	400
3	1.18	4.2	3.8	400
4	1.40	4.5	3.5	400
5	1.70	4.9	3.1	400
6	2.00	5.2	2.8	400

3. Results and discussion

3.1. Synthetic products identification

3.1.1. XRD

XRD test results of synthetic products are described in Fig. 3. The identical peaks with the d-spacing of 3.04, 2.79, 1.82, 1.66 Å indicate that the C-S-H phase synthesized in this study is similar to C-S-H (I), which is one of the C-S-H phases found in the Portland cement concrete[13]. Due to the high reactivity of fumed silica, the C-S-H phases can be formed after 2 weeks' reaction, see Fig. 3 (a). When the designed C/S is less than 1.40, only C-S-H phase exists in the product with no trace of unreacted raw materials or carbonation product; otherwise, the portlandite appears, see Fig.2 (b). This is consistent with other researchers' results[14, 15].

3.1.2. NMR

The NMR test results of synthetic products are described in Fig. 4a and 4b. The peaks around -78 ppm and -85 ppm indicates the Q^1 and Q^2 type of tetrahedra respectively. Apparently, the peak intensity of Q^1 increases with the increase of the C/S while that of Q^2 decreases.

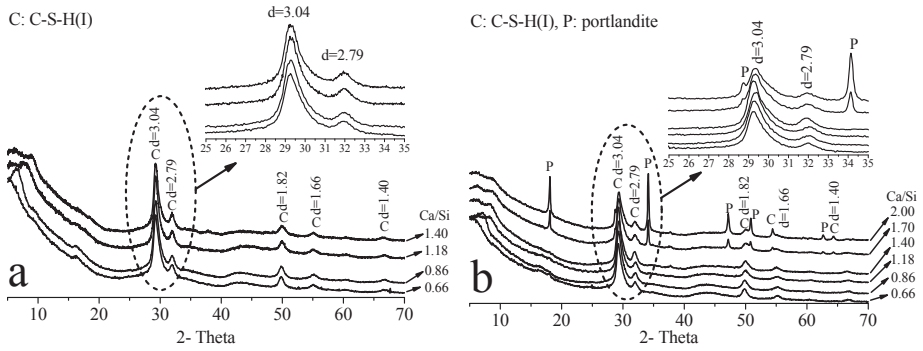

Figure 3 XRD test results of C-S-H with different C/S (0.66-2.0). C-S-H d-spacings are noted above their respective peaks in the units of Ångstrom (Å). a- synthesis for 2 weeks; b- synthesis for 4 weeks.

The increase of C/S in C-S-H can be caused by the omission of the bridge tetrahedra in the silicate chain, based on the structure of tobermorite. The consequence is the decrease of the proportion of Q^2 tetrahedra and the formation of more Q^1 tetrahedra. Moreover, the mean silicate chain length (MCL) will decrease. The MCL was calculated from the NMR data using Eq. (2).

$$MCL = \frac{2(Q^1 + Q^2)}{Q^1} \tag{2}$$

In which, the Q^1 and Q^2 indicate the fractions of Si present in Q^1 and Q^2 tetrahedra respectively. Quantitative information on the fractions of Q^1, Q^2 tetrahedra was obtained by the deconvolution of the single pulse spectra. The spectra were fitted to Gaussian/Lorentzian

mixed function using the dmfit2015 software. The fitting result of an example is illustrated in Fig. 5.

The deconvolution process is performed on all the ^{29}Si NMR test results of C-S-H with C/S ranging from 0.66 to 2.0. The MCL is calculated and plot with the C/S, comparing with the results from other researches of synthesized C-S-H in the solution[13, 16-20], see Fig. 6.

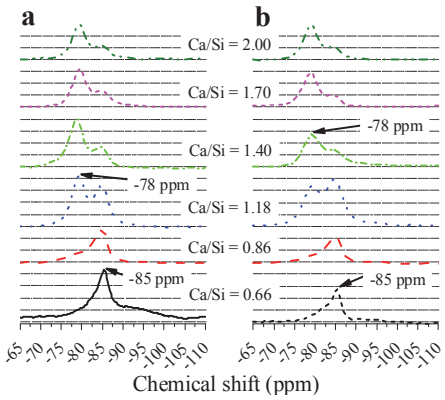

Figure 5 ^{29}Si NMR test results of C-S-H with different C/S (0.66-2.0), a- synthesis for 2 weeks; b-synthesis for 4 weeks.

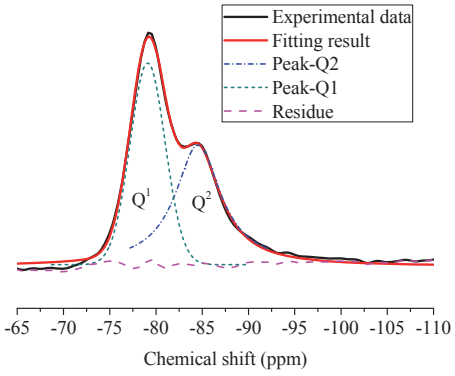

Figure 4 Fitting results of 29Si NMR spectrum (Ca/Si = 1.4, synthesis for 4 weeks).

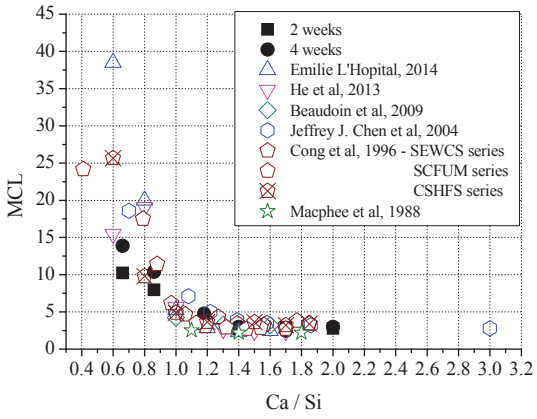

Figure 6 Calculated mean silicate chain length (M CL) of C-S-H with different C/S.

The MCL of the C-S-H decreases with the increasing C/S when the C/S is lower than 1.4. Then the MCL stays at around 2~3 tetrahedron units long. This can just verify the evolution model of C-S-H with higher C/S based on the tobermorite (Ca/Si = 0.83). By omission the bridge tedrahedra, the C/S will increase; meanwhile, the long silicate chain will be broken into shorter polymeric species of SiO_4 terdrahedra. Therefore, the MCL of C-S-H decreases

with the increase of the C/S. The C/S increases to 1.25 by the omission of all the bridge tetrahedra in the silicate chain. The further incorporation of Ca in the interlayer can achieve the C/S of 1.4, which will not affect the MCL. This is why the MCL of C-S-H keeps unchanged when the C/S increases above 1.4. The structure of C-S-H with the C/S higher than 1.4 can be explained by the 'T/CH' model, a 'solid solution' of C-S-H and CH.

Results in Fig. 6 also prove that the C/S of the synthetic C-S-H is quite close to the designed value. Considering together with the XRD test results, the conclusion can be made that the single C-S-H (I) phase with different C/S (lower than 1.4) is successfully synthesized in this research, and the experiment set-up can prevent the carbonation effectively.

3.2. Carbonation of C-S-H with different C/S

To avoid the effects from the carbonation of portlandite, only the C-S-H with the C/S of 0.66 to 1.40 were used in the carbonation study. The carbonation product was analyzed by NMR and FTIR. The results are shown and discussed as follows.

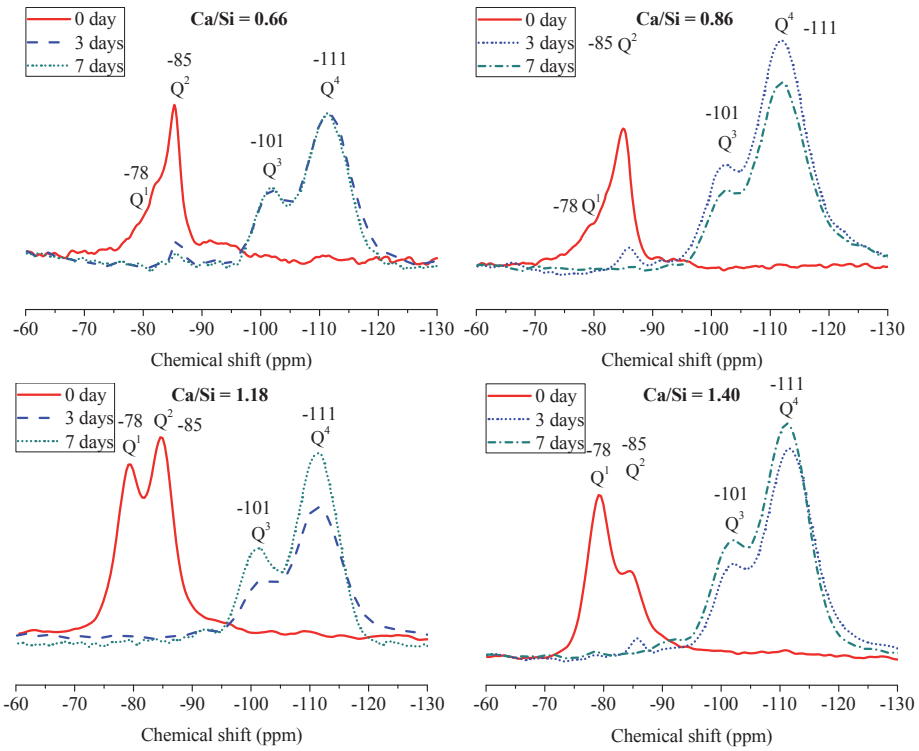

Figure 7 NMR test results of different types of C-S-H, carbonated for different time.

The ^{29}Si NMR test results of carbonated C-S-H with different C/S are shown in Fig. 7. The characteristic peaks at around -101 and -111 ppm indicate the Q^3 and Q^4 tetrahedra, respectively. After carbonation, the fraction of Q^3 and Q^4 tetrahedra increases while the

fraction of Q^1 and Q^2 tetrahedra decreases at the same time. This indicate the polymerization process of the silicate chain and the removal of Ca in the CaO_2 sheet layer. The consequence is the linkage of the adjacent silicate chains and to form the silicate network in two and three dimensions. Whatever the C/S is, the silicate in the final carbonation products of C-S-H is silica gel, not the mixture or 'solid solution' of $CaCO_3$ and C-S-H with lower C/S[21].

Although the alkalinity of C-S-H is much lower than portlandite, the carbonation of C-S-H is quite faster under the accelerated condition. Nearly all the C-S-H are decomposed into silica gel after 3 days' carbonation.

In the FTIR spectra of C-S-H, there is a characteristic peak at around 970 cm^{-1}. This peak indicates the Si-O stretching vibrations of Q^2 tetrahedra, which shifts to the lower frequency with increasing of C/S[22]. In the contrary, the position of this peak shifts to the higher frequency. The FTIR tests were performed on the C-S-H with the C/S of 0.66 to 1.40. The carbonation time varied from 0.5 h to 24 h. The test results are compared in Fig. 8.

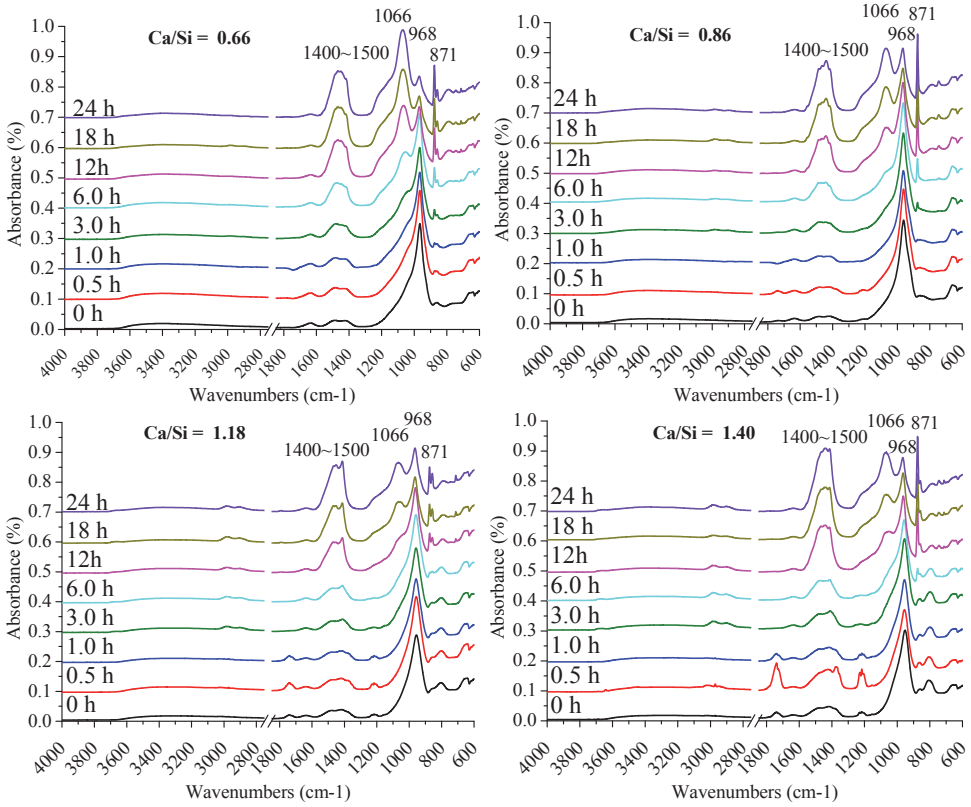

Figure 8 FTIR test results of different types of C-S-H, carbonated for different time

The shoulder peak at around 1066 cm^{-1}, which is also indicating to the Si-O stretching vibrations of Q^2 tetrahedra, has an obvious growth after carbonation. This peak only appears

in the FTIR spectrum of C-S-H with low C/S or in the tobermorite. Meanwhile, the intensity of the peak at around 970 cm^{-1} decreases dramatically. The changes of these two peaks during the carbonation reveal the progressive polymerization of silicate chains.

The peak at around 875 and 1400~1500 cm^{-1} represents the bending (v2) of CO_3^{2-} and the stretching (v3) of CO_3^{2-}, respectively. Both of them have a dramatic increase in the intensity when the shoulder peak (1066 cm^{-1}) grows into an obvious and independent peak. For example, it can be observed in the spectrum when the C-S-H with the C/S of 0.66 is carbonated for 3 h. This 'critical' time is 6h for the C-S-H with the C/S of 0.86 and 12 h for the rest two types of C-S-H. This change in the FTIR spectra indicates that the silicate chain in the C-S-H starts to be destructed by the carbonation. Comparing this "start time" among different types of C-S-H, it can be concluded that the carbonation rate of the C-S-H with a higher C/S is lower than that of the C-S-H with the lower C/S. High Ca C-S-H has a better resistance to the carbonation.

4. Conclusions

In the paper, the C-S-H with different C/S, identified by XRD and ^{29}Si NMR, is successfully synthesized from CaO and fumed silica in the solution protected by the N_2 flow. The carbonation mechanism of C-S-H including final products and rate are studied by NMR and FTIR. The carbonation resistance among different types of C-S-H are discussed. The main conclusions are as follow:

- The single phase of C-S-H(I) can be synthesized when the Ca/Si ratio is no more than 1.40; otherwise the portlandite appears.
- The structure of C-S-H with the C/S lower than 1.25 can be derived by missing the bridge tedrahedra based on tobermorite; the incorporation of extra Ca^{2+} can achieve a much higher C/S of 1.40; The structure of C-S-H with the C/S higher than 1.4 can be explained by the 'T/CH' model, a 'solid solution' of C-S-H and CH.
- The final silicate in the products is silicate gel. The C-S-H with high C/S has the better resistance to the carbonation.

Acknowledgements

The authors are grateful for the help from technicians and experimental supports from Microlab, Delft University of Technology.

References

[1] Black L., et al., Structural features of C–S–H (I) and its carbonation in air—a Raman spectroscopic study. Part II: carbonated phases, J Am Ceram Soc, 90 (2007) 908-917.
[2] Morandeau A., et al., Investigation of the carbonation mechanism of CH and CSH in terms of kinetics, microstructure changes and moisture properties, Cement Concrete Res, 56 (2014) 153-170.

[3] Merlino S., et al., The real structure of tobermorite 11Å normal and anomalous forms, OD character and polytypic modifications, Eur J Mineral, 13 (2001) 577-590.
[4] Megaw H. D., Kelsey C. H., Crystal Structure of Tobermorite, Nature, 177 (1956) 390-391.
[5] Mohan K., Taylor H., A trimethylsilylation study of tricalcium silicate pastes, Cement Concrete Res, 12 (1982) 25-31.
[6] Dent Glasser L. S., et al., Identification of some of the polysilicate components of trimethylsilylated cement paste, Cement Concrete Res, 11 (1981) 775-780.
[7] Dent Glasser L. S., et al., A Multi-Method Study of C15 Hydration, Cement Concrete Res, 8 (1978) 7.
[8] Manzano H., et al., Aluminum incorporation to dreierketten silicate chains, The Journal of Physical Chemistry B, 113 (2009) 2832-2839.
[9] Richardson I., Tobermorite/jennite-and tobermorite/calcium hydroxide-based models for the structure of CSH: applicability to hardened pastes of tricalcium silicate, β-dicalcium silicate, Portland cement, and blends of Portland cement with blast-furnace slag, metakaolin, or silica fume, Cement Concrete Res, 34 (2004) 1733-1777.
[10] Taylor H., Howison J., Relationships between calcium silicates and clay minerals, Clay Minerals Bull, 3 (1956) 98-111.
[11] Chen J. J., et al., Decalcification shrinkage of cement paste, Cement Concrete Res, 36 (2006) 801-809.
[12] Wu B., Ye G., Development of porosity of cement paste blended with supplementary cementitious materials after carbonation, 14th International Congress on the Chemistry of Cement (ICCC2015), 2015, pp. 1-18.
[13] Chen J. J., et al., Solubility and structure of calcium silicate hydrate, Cement Concrete Res, 34 (2004) 1499-1519.
[14] Renaudin G., et al., Structural characterization of C–S–H and C–A–S–H samples—Part I: Long-range order investigated by Rietveld analyses, Journal of Solid State Chemistry, 182 (2009) 3312-3319.
[15] Garbev K., et al., Cell Dimensions and Composition of Nanocrystalline Calcium Silicate Hydrate Solid Solutions. Part 1: Synchrotron-Based X-Ray Diffraction, J Am Ceram Soc, 91 (2008) 3005-3014.
[16] Macphee D., et al., Polymerization effects in CSH: implications for Portland cement hydration, Adv Cem Res, 1 (1988) 131-137.
[17] Cong X. D., Kirkpatrick R. J., Si-29 MAS NMR study of the structure of calcium silicate hydrate, Adv Cem Based Mater, 3 (1996) 144-156.
[18] Beaudoin J. J., et al., A< sup> 29</sup> Si MAS NMR study of modified C–S–H nanostructures, Cement and Concrete Composites, 31 (2009) 585-590.
[19] He Y., et al., Effect of calcium–silicon ratio on microstructure and nanostructure of calcium silicate hydrate synthesized by reaction of fumed silica and calcium oxide at room temperature, Mater Struct, (2013) 1-12.
[20] L'Hôpital É. M., Aluminium and alkali uptake in calcium silicate hydrates (C-S-H), PhD thesis, EPFL(2014).
[21] Papadakis V. G., et al., A reaction engineering approach to the problem of concrete carbonation, AIChE Journal, 35 (1989) 1639-1650.
[22] Yu P., et al., Structure of Calcium Silicate Hydrate (C‐S‐H): Near‐, Mid‐, and Far‐Infrared Spectroscopy, J Am Ceram Soc, 82 (1999) 742-748.